Computational Study of the Hanbury Brown and Twiss Effect

Matthew Belzer

Laser Teaching Center

Department of Physics and Astronomy, Stony Brook University

Stony Brook, NY 11794

May 20, 2021

Abstract

In 1956, Robert Hanbury Brown and Richard Q. Twiss observed intensity correlations from visible light that was produced by an incoherent source [1]. This experiment marked the birth of intensity interferometry for visible wavelengths and in 1956 they applied their findings to measure the diameter of the star Sirius [2]. Additionally, this experiment inspired the foundation of quantum optics and has been used as evidence of photon bunching [3]. I have investigated their results by using Python to simulate the emission of light with a randomized phase from two incoherent point sources. The light from each source propagates to two detectors with a variable distance between them. I observed that the second order correlation depended on the distance between the detectors sinusoidally, which was what we expected from the analytic result. I generalized this two point simulation by simulating the intensity correlation that comes from a star. My results matched what they found in their Sirius paper [2].

Contents

1 Introduction

Light that travels in the $\vec{k}$ direction has an electric field amplitude described by

$$E(\vec{r},t) = E_0 e^{i(\vec{k}\cdot\vec{r}-\omega t+\phi)} \tag{1}$$

where E_0 is the amplitude of the wave, $\vec{k}$ is the wave vector, $\vec{r}$ is a point in space, t is the time, ω is the angular frequency, and ϕ is the phase. The irradiance of the light, I, is proportional to $E(\vec{r},t)$ multiplied with its complex conjugate

$$I(\vec{r},t) \propto E(\vec{r},t)E^*(\vec{r},t) = E_0 e^{i(\vec{k}\cdot\vec{r}-\omega t+\phi)} E_0 e^{-i(\vec{k}\cdot\vec{r}-\omega t+\phi)} = E_0^2 \tag{2}$$

Typically, I is thought to be the intensity but this is incorrect [4]. In actuality, the intensity is the power per unit solid angle per unit area, where a solid angle is the 3D equivalent to a two dimensional angle [4]. The irradiance on the other hand, is the power per unit area [4]. However, in the case of this paper, there is no meaningful difference between the two because the constants that differentiate them cancel out when the math is done.

The degree of spatial coherence between two point sources (1 and 2) can be calculated using the first order correlation function

$$g^{(1)} = \frac{\langle E_1(\vec{r_1},t)E_2^*(\vec{r_2},t)\rangle}{\sqrt{I_1 I_2}} \tag{3}$$

where E_1 and E_2 are the amplitudes at the first point ($\vec{r_1}$) and the second point ($\vec{r_2}$) and I_1 and I_2 are the intensities at the first and second points respectively [4]. The angular brackets in the numerator denote a time average. This is known as a first order correlation [4]. The denominator normalizes the numerator so that the range of the correlation is [-1, 1]. If $|g^{(1)}| = 1$ the light is completely coherent, but if $|g^{(1)}| = 0$, the light is completely incoherent. Otherwise, it is said that the light is partially coherent. The degree of coherence of light can physically be measured using fringe visibility.

The second order correlation, which is also known as the intensity correlation, measures the correlation between the intensities at two points [5].

$$g^{(2)} = \frac{\langle I_1 I_2\rangle}{\langle I_1\rangle\langle I_2\rangle} \tag{4}$$

Intensity correlations differ from first order correlations because their range is [0,2]. Additionally, the first order correlation is impacted by phase, but the second order correlation is not since the phase of the light cancels out when calculating the time averaged intensity at a point.

Hanbury Brown and Twiss (HBT) successfully measured the intensity correlation of visible light emitted

from an incoherent source [1]. They used the apparatus in Figure 1, where they filtered an incoherent mercury arc lamp to isolate mercury's 435.8 nm wavelength [1]. The light that passed through the filters then went through a beamsplitter to be detected by two photomulitplier tubes (PMTs) [1]. The PMTs outputted a fluctuating current which was used to measure the intensity correlation of the source [1].

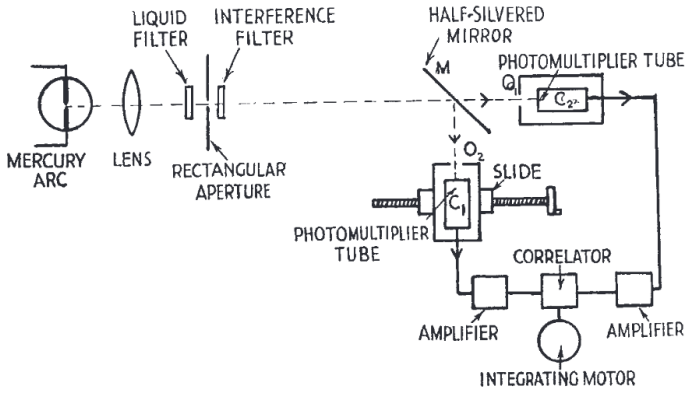

Figure 1: HBT's tabletop experiment design [1].

There was a lot of controversy surrounding this result because many physicists doubted that converting the photons into a photocurrent and measuring the fluctuations preserves the intensity correlation [6], [7]. Specifically, one group of researchers tried to recreate the experiment and found that the rate of photoelectron coincidences was comparable to the random rate [6]. This discrepancy came from how their beam of light went through a pinhole was then divided into two coherent beams using a beamsplitter [6]. HBT mathematically demonstrated that this result was to be expected from this key difference [6]. Another detractor said that the semiclassical assumptions that they made were invalid [7]. In this case too, they were able to demonstrate that their assumptions were correct and agreed with quantum mechanics [7].

Before the HBT experiment, intensity correlations have been used for radio wavelengths to measure the angular diameter of stars [2]. However for nearby stars, to accurately measure the angular diameter would require baselines that are on the order of hundreds to thousands of kilometers apart, which is highly impractical. Using light in the visible range, like HBT did in their tabletop experiment, limits the baselines to ranges on the order of tens and hundreds of meters which is more feasible [2]. Intensity intereferometry was also advantageous to use for these nearby stars because of its great resolving power, the measurements being limited by electronic rather than optical equipment, and atmospheric scintillation having no affect on the correlation measurements [2]. Therefore, HBT built an intensity interferometer to measure the angular diameter of Sirius using visible wavelengths (see Figure 2). They did this by collecting light into two photocells using two mirrors and, like in their tabletop experiment, they correlated the emitted photocurrents.

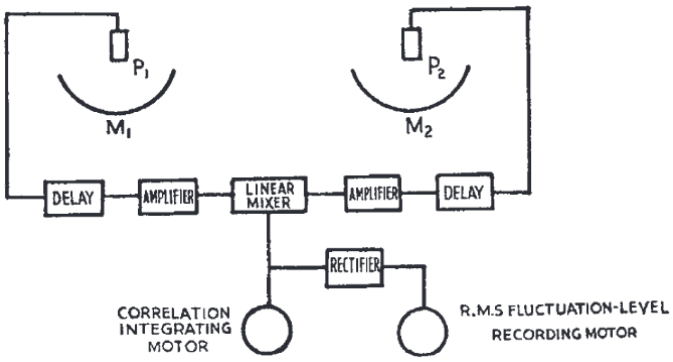

Figure 2: HBT's Sirius experimental design [2]

To determine the angular diameter θ_{UD} of the star, HBT assumed that the star is a uniform circular disk and they derived the intensity correlation to be

$$g^{(2)} = 1 + \left[\frac{2J_1(\pi\theta_{UD}d/\lambda)}{\pi\theta_{UD}d/\lambda}\right]^2 \tag{5}$$

where $J_1(x)$ is the first order Bessel Function and d is the distance between the detectors. Using this method, they got a reasonable angular diameter of .0068" $\pm$ .0005", which was close to the theoretical value of .0063" [2].

1.1 Two Point Sources

There is an analytic solution for the intensity correlation between two incoherent point sources (A and B) that emit light to two detectors (1 and 2) [5] (see Figure 3).

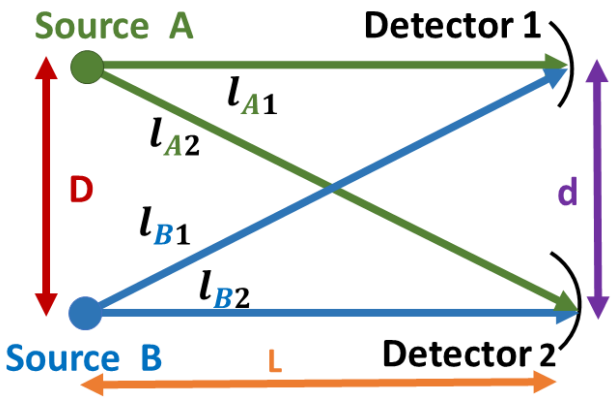

Figure 3: The two source, two detector condition.

The sources are separated by a distance D and the detectors are separated by a distance d. The sources

and detectors are separated by a distance L. The paths between each detector and each source are described by $l_{\text{Source Detector}}$. The light emitted from Source A has a phase of ϕ_a and an amplitude of a and the light emitted from Source B has a phase of ϕ_b and an amplitude of b. Therefore, the amplitudes at Detectors 1 and 2 are described by

$$E_1 = ae^{i(kl_{A1}+\phi_a)} + be^{i(kl_{B1}+\phi_b)} \tag{6}$$

$$E_2 = ae^{i(kl_{A2}+\phi_a)} + be^{i(kl_{B2}+\phi_b)} \tag{7}$$

I have ignored the time terms in the amplitudes because they can essentially be included in the phase term [5]. Using Eq. 2, the subsequent intensities are

$$I_1 = a^2 + b^2 + abe^{i(k(l_{A1}-l_{B1})+\phi_b-\phi_a)} + abe^{-i(k(l_{A1}-l_{B1})+\phi_b-\phi_a)} \tag{8}$$

$$I_2 = a^2 + b^2 + abe^{i(k(l_{A2}-l_{B2})+\phi_b-\phi_a)} + abe^{-i(k(l_{A2}-l_{B2})+\phi_b-\phi_a)} \tag{9}$$

Since there is a random phase difference in each of the exponential terms, when the intensities are individually time averaged those terms go to zero. This happens because across a large enough time frame, the phases will change infinitely many times since it is an incoherent source. This averaging yields

$$\langle I_1 \rangle = \langle I_2 \rangle = a^2 + b^2 \tag{10}$$

The product of the intensities is

$$\begin{aligned} I_1 I_2 = {} & (a^2+b^2)^2 + a^3be^{i(k(l_{A1}-l_{B1})+\phi_b-\phi_a)} + a^3be^{-i(k(l_{A1}-l_{B1})+\phi_b-\phi_a)} + ab^3e^{i(k(l_{A1}-l_{B1})+\phi_b-\phi_a)} \\ & + ab^3e^{-i(k(l_{A1}-l_{B1})+\phi_b-\phi_a)} + a^3be^{i(k(l_{A2}-l_{B2})+\phi_b-\phi_a)} + a^3be^{-i(k(l_{A2}-l_{B2})+\phi_b-\phi_a)} + ab^3e^{i(k(l_{A2}-l_{B2})+\phi_b-\phi_a)} \\ & + ab^3e^{-i(k(l_{A2}-l_{B2})+\phi_b-\phi_a)} + a^2b^2e^{i(k(l_{A1}-l_{B1})+\phi_b-\phi_a+k(l_{A2}-l_{B2})+\phi_b-\phi_a)} \\ & + a^2b^2e^{-i(k(l_{A1}-l_{B1})+\phi_b-\phi_a+k(l_{A2}-l_{B2})+\phi_b-\phi_a)} \\ & + \boxed{a^2b^2e^{i(k(l_{A1}-l_{B1}-l_{A2}+l_{B2}))} + a^2b^2e^{-i(k(l_{A1}-l_{B1}-l_{A2}+l_{B2}))}} \end{aligned} \tag{11}$$

The last two terms are the most important terms because the phases cancel out, leaving only constant terms. When I time averaged the product of the intensities and used the identity $e^{ix} + e^{-ix} = 2\cos(x)$, I get

$$\begin{aligned} \langle I_1 I_2 \rangle &= (a^2+b^2)^2 + a^2b^2e^{i(k(l_{A1}-l_{B1}-l_{A2}+l_{B2}))} + a^2b^2e^{-i(k(l_{A1}-l_{B1}-l_{A2}+l_{B2}))} \\ &= (a^2+b^2)^2 + 2a^2b^2\cos(k(l_{A1}-l_{B1}-l_{A2}+l_{B2})) \end{aligned} \tag{12}$$

Plugging these equations into Eq. 4, I get

$$g^{(2)} = \frac{(a^2+b^2)^2 + 2a^2b^2\cos(k(l_{A1} - l_{B1} - l_{A2} + l_{B2}))}{(a^2+b^2)^2} = 1 + \frac{2a^2b^2\cos(k(l_{A1} - l_{B1} - l_{A2} + l_{B2}))}{(a^2+b^2)^2} \tag{13}$$

which shows that the path length that the light travels has a sinusoidal affect on the intensity correlation in a two source, two detector system.

For the case of $L \gg D$, an approximation can be made [5]. To do this, I define the distances between the sources and the detectors as vectors (see Figure 4). I also define vectors $\vec{r_1}$ and $\vec{r_2}$ to go from detectors 1 and 2 respectfully to the midpoint between the two sources. From that midpoint, I draw two more vectors that go to Source A and Source B and label them $\vec{D}/2$ and $-\vec{D}/2$ respectfully since they are half the value of D in the original diagram.

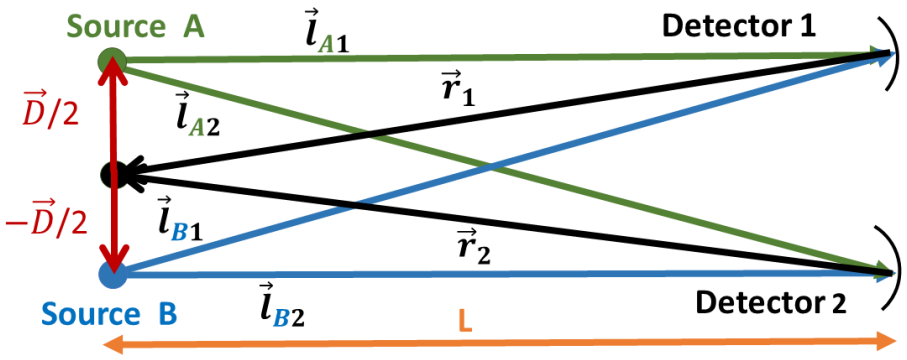

Figure 4: Vector diagram for the small angle approximation.

Using these new vectors, I can define $\overrightarrow{l_{A2}}$ as

$$\overrightarrow{l_{A2}} = -\frac{\vec{D}}{2} - \vec{r_2} \tag{14}$$

The square of the magnitude of this is

$$\overrightarrow{l_{A2}}^2 = \left(-\frac{\vec{D}}{2} - \vec{r_2}\right) \cdot \left(-\frac{\vec{D}}{2} - \vec{r_2}\right) = \frac{\vec{D}\cdot\vec{D}}{4} + \vec{D}\cdot\vec{r_2} + \vec{r_2}\cdot\vec{r_2} \approx \vec{D}\cdot\vec{r_2} + \vec{r_2}\cdot\vec{r_2} \tag{15}$$

Since $L \gg D$, that means that the $\frac{\vec{D}\cdot\vec{D}}{4}$ term is much smaller than the other terms since $\vec{r_2} \gg \vec{D}$ is a consequence of the other inequality. Finding the square root of Eq. 15 gives me

$$\sqrt{\overrightarrow{l_{A2}}^2} = l_{A2} = \sqrt{\vec{D}\cdot\vec{r_2} + \vec{r_2}\cdot\vec{r_2}} = r_2\sqrt{1 + \frac{\hat{r_2}\cdot\vec{D}}{r_2}} \approx r_2 + \frac{\hat{r_2}\cdot\vec{D}}{2} \tag{16}$$

The final equation comes from the approximation $(1+x)^n \approx 1+nx$ and in this case $n = .5$. Using the same process, equivalent values can be found for the rest of the path lengths.

$$l_{A1} \approx r_1 + \frac{\hat{r_1} \cdot \vec{D}}{2} \tag{17}$$

$$l_{B1} \approx r_1 - \frac{\hat{r_1} \cdot \vec{D}}{2} \tag{18}$$

$$l_{B2} \approx r_2 - \frac{\hat{r_2} \cdot \vec{D}}{2} \tag{19}$$

Plugging these terms back into the cosine argument of Eq. 13 yields

$$\begin{aligned} k(l_{A1} - l_{B1} - l_{A2} + l_{B2}) &= k\left(r_1 + \frac{\hat{r_1} \cdot \vec{D}}{2} - r_2 - \frac{\hat{r_2} \cdot \vec{D}}{2} - r_1 + \frac{\hat{r_1} \cdot \vec{D}}{2} + r_2 - \frac{\hat{r_2} \cdot \vec{D}}{2}\right) \\ &= k(\hat{r_1} \cdot \vec{D} - \hat{r_2} \cdot \vec{D}) = \vec{D} \cdot (\hat{r_1} - \hat{r_2})k = \vec{D} \cdot (\vec{k_1} - \vec{k_2}) \end{aligned} \tag{20}$$

where $\vec{k_i} = k\vec{r_i}$. Plugging this argument back into Eq. 13 gives me

$$g^{(2)} = 1 + \frac{2a^2b^2\cos(\vec{D} \cdot (\hat{k_1} - \hat{k_2}))}{(a^2+b^2)^2} \tag{21}$$

An important note to make is that the oscillations of the cosine term will be most easily observed on a detector separation of $d = \lambda/\theta$ where $\theta = R/L$ is the angular separation between the two points [5]. This relationship recalls the Fraunhofer diffraction result in Eq. 5, since this equation is similar to the equation for the radius of an Airy disk's first dark ring [4]. Where Airy disks are the diffraction patterns that emerge from circular apertures [4].

1.2 N_S Point Sources

The intensity correlation for N_S point sources can be thought of as the superposition of all of the intensity correlations between all of the pairs of sources. To demonstrate this, I found the solution for the intensity correlation of a three point source, two detector system. The light emitted from sources A, B, and C will have amplitudes of a, b, and c respectively. The phases from sources A, B, and C will be ϕ_a, ϕ_b, and ϕ_c The distance between the sources and detectors will be done using the same nomenclature as Section 1.1. The amplitudes of detectors 1 and 2 are

$$E_1 = ae^{i(kl_{A1}+\phi_a)} + be^{i(kl_{B1}+\phi_b)} + ce^{i(kl_{C1}+\phi_c)} \tag{22}$$

$$E_2 = ae^{i(kl_{A2}+\phi_a)} + be^{i(kl_{B2}+\phi_b)} + ce^{i(kl_{C2}+\phi_c)} \tag{23}$$

The intensities are therefore

$$\begin{aligned} I_1 = {} & a^2 + b^2 + c^2 + abe^{i(k(l_{A1}-l_{B1})+\phi_b-\phi_a)} + abe^{-i(k(l_{A1}-l_{B1})+\phi_b-\phi_a)} \\ & + ace^{i(k(l_{A1}-l_{C1})+\phi_c-\phi_a)} + ace^{-i(k(l_{A1}-l_{C1})+\phi_b-\phi_a)} \\ & + bce^{i(k(l_{B1}-l_{C1})+\phi_c-\phi_b)} + bce^{-i(k(l_{B1}-l_{C1})+\phi_b-\phi_c)} \end{aligned} \tag{24}$$

$$\begin{aligned} I_2 = {} & a^2 + b^2 + c^2 + abe^{i(k(l_{A2}-l_{B2})+\phi_b-\phi_a)} + abe^{-i(k(l_{A2}-l_{B2})+\phi_b-\phi_a)} \\ & + ace^{i(k(l_{A2}-l_{C2})+\phi_c-\phi_a)} + ace^{-i(k(l_{A2}-l_{C2})+\phi_b-\phi_a)} \\ & + bce^{i(k(l_{B2}-l_{C2})+\phi_c-\phi_b)} + bce^{-i(k(l_{B2}-l_{C2})+\phi_b-\phi_c)} \end{aligned} \tag{25}$$

The time averages of the intensities are just the constants since the exponentials have a random phase

$$\langle I_1 \rangle = \langle I_2 \rangle = a^2 + b^2 + c^2 \tag{26}$$

This is very similar to Eq. 10, except there is an additional amplitude square. So, this can be generalized for n points to just being the sum of the squares of the amplitude coefficients.

I used Mathematica to find the product of the intensities in Eq. 24 and 25 since there are 9^2 terms (see Figure 5). The naming convention is slightly different for my Mathematica results. The amplitudes are labelled the same, but their respective phases are pa, pb, and pc, not ϕ. I also dropped the l and made the subscript the distances between the sources and detectors, so the distance between Source B and Detector 1 is $B1$ instead of l_{B1}.

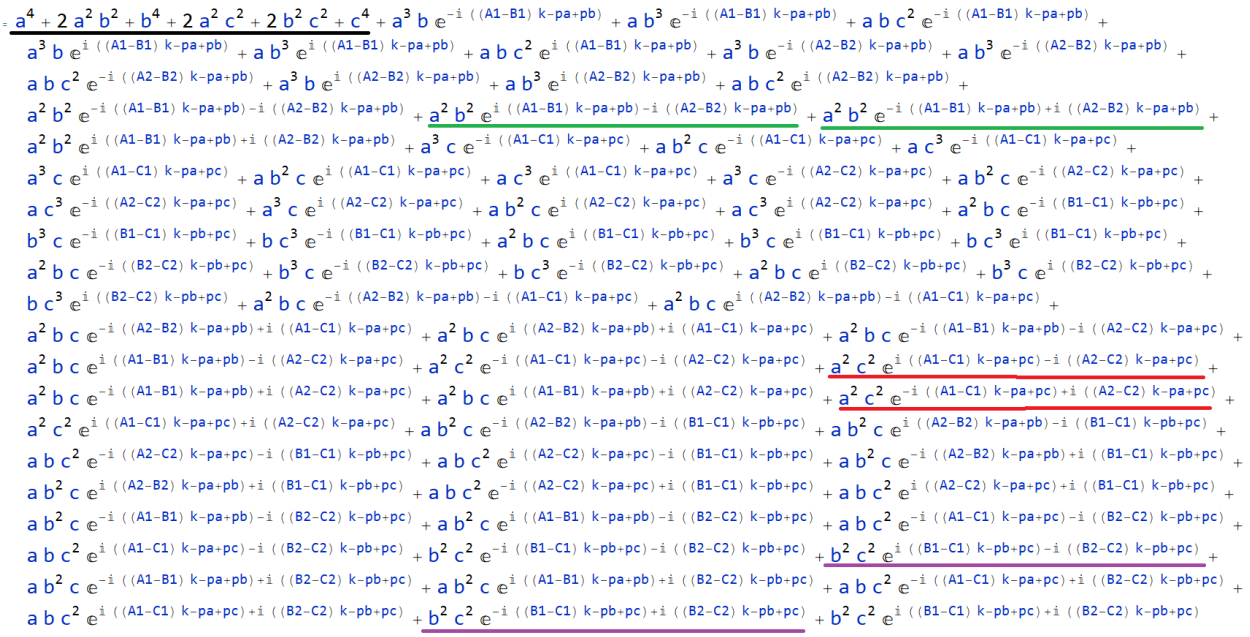

Figure 5: The three source and two detector system $I_1 \times I_2$ expansion.

The term underlined in black is all of the constants and can be rewritten as $(a^2+b^2+c^2)^2$. Due to the identity of $e^{ix}+e^{-ix} = 2\cos(x)$, the terms underlined in green can be rewritten as $2a^2b^2\cos(k(l_{A1}-l_{B1}-l_{A2}+l_{B2}))$. Similarly, the terms underlined in red and purple can be rewritten as $2a^2c^2\cos(k(l_{A1}-l_{C1}-l_{A2}+l_{C2}))$. and $2b^2c^2\cos(k(l_{B1}-l_{C1}-l_{B2}+l_{C2}))$ respectively. These terms are important because their phases cancel out and the rest of the terms go to zero when the time average is done. Hence,

$$\begin{aligned}\langle I_1 I_2\rangle = (a^2+b^2+c^2)^2 + 2a^2b^2\cos(k(l_{A1}-l_{B1}-l_{A2}+l_{B2})) + 2a^2c^2\cos(k(l_{A1}-l_{C1}-l_{A2}+l_{C2}))\\ + 2b^2c^2\cos(k(l_{B1}-l_{C1}-l_{B2}+l_{C2}))\end{aligned} \tag{27}$$

Therefore, the resulting second order correlation is in the form of

$$\begin{aligned}g^{(2)} = \frac{(a^2+b^2+c^2)^2 + 2a^2b^2\cos(k(l_{A1}-l_{B1}-l_{A2}+l_{B2})) + 2a^2c^2\cos(k(l_{A1}-l_{C1}-l_{A2}+l_{C2}))}{(a^2+b^2+c^2)^2}\\ + \frac{2b^2c^2\cos(k(l_{B1}-l_{C1}-l_{B2}+l_{C2}))}{(a^2+b^2+c^2)^2} = 1 + 2\frac{a^2b^2\cos(k(l_{A1}-l_{B1}-l_{A2}+l_{B2}))}{(a^2+b^2+c^2)^2}\\ + 2\frac{a^2c^2\cos(k(l_{A1}-l_{C1}-l_{A2}+l_{C2})) + b^2c^2\cos(k(l_{B1}-l_{C1}-l_{B2}+l_{C2}))}{(a^2+b^2+c^2)^2}\end{aligned} \tag{28}$$

For the case of N_S sources, this can be generalized to

$$g^{(2)} = 1 + 2\frac{a^2b^2\cos(k(l_{A1} - l_{B1} - l_{A2} + l_{B2})) + a^2c^2\cos(k(l_{A1} - l_{C1} - l_{A2} + l_{C2}))}{(a^2 + b^2 + c^2 + ...)^2} + 2\frac{b^2c^2\cos(k(l_{B1} - l_{C1} - l_{B2} + l_{C2})) + ...}{(a^2 + b^2 + c^2 + ...)^2} \tag{29}$$

where the numerator of the fraction is all of the combinations of path differences and source amplitudes using that sign convention and the denominator is the sum of the squares of all the source amplitudes. It is important to note that there should be C(N_S, 2) cosine terms in the numerator since the cosine terms are combinations of sources. To show that this is true, for two sources, there is one cosine term and C(2,2) = 1 and for three sources, there are three cosine terms and C(3,2) = 3.

2 Computational Methods

The full simulation code can be viewed on GitHub:
https://github.com/MatthewBelzer/HBT-Simulations.

2.1 Two Point Sources

To simulate the intensity correlations, I considered light with randomly generated phases differences from two sources N_p times and found the intensity correlation for each iteration and averaged it. This was done for N_d discrete distances between 0 and d. A more detailed explanation of the code can be found below

1. Give values to the following constants: the wave number k, the positions of the sources, the number of random phases N_p, the number of detector distances N_d, and the range of the detector distances.
2. For the N_d distances in the distance array:
   (a) Calculate the distances between the sources and the detectors.
   (b) Find the theoretical value using Eq. 13
   (c) For N_p phase differences in the randomly generated phase array:
      i. Use Eq. 1 and 2 to find the amplitudes and the intensities at each of the detectors.
      ii. Correlate these intensities using Eq. 4.
   (d) Average the correlations across all of the phases.

For the simulation, k was set to 10^8 rad/m, there were 100 distances calculated (N_d), and there were 1000 random phase differences between 0 and 2π (N_p). The amplitudes for both sources were set to 1. The

positions of Source A and Source B were (0, 100) m and (0, -100) m respectively. The positions of detectors 1 and 2 were (10^6, $d/2$) m and (10^6, $-d/2$) m respectively, where d ranged between 0 and 1 mm.

2.2 N_S Point Sources on a Star

To verify HBT's Sirius results, I generated N_S points on the surface of a hemisphere facing the detectors so that all of those sources appear like a star. The rest of the simulation was the practically the same as the two point simulation except that I generalized the distances and the random phases using arrays. A description of my code can be found below

1. Give values to the following constants: the wave number k, the number of random phases N_p, the number of detector distances N_d, the range of the detector distances, number of sources N_S, y distance from the midpoint of the detectors to the surface of the star, and star radius R.
2. Generate N_S points on the surface of a star facing my detector positions
3. For the N_d distances in the distance array:
   (a) For N_S Sources:
      i. Calculate the distance from each source to each detector
   (b) Find the theoretical value using Eq. 29
   (c) For N_p phases:
      i. Generate a phase array that has a phase for each of the N_S sources
      ii. Use Eq. 1 and 2 to find the amplitudes and the intensities at each of the detectors.
      iii. Correlate these intensities using Eq. 4.
   (d) Average the correlations across all of the phases.

I generated sources on the surface of the star using two methods. The first method was randomized and the second method used an algorithm that generated a Fibonacci Sphere, which makes the points roughly equidistant form each other [8].

An important part of my code that I want to highlight is my method of calculating the theoretical curve. I used a recursive method where I found the cosine numerator terms between the first source and all other sources. Next I removed the first source from my distance arrays and found the cosine terms for the second source and all other sources. I then removed the second source from my distance arrays and found the cosine terms for the third source and all other sources. I repeated this until I had one source left in the array. This method lets me find the theoretical curve for any number of N_S sources.

For my first simulations, k was set to 10^8 rad/m, there were 100 distances calculated (N_d), and there were 2000 random phase differences between 0 and 2π (N_p). The amplitudes for all of the sources were set to 1. I generated 1000 sources on the surface of a hemisphere of Radius 100m that's center was 1000 km away from the midpoint of the detectors. The positions of detectors 1 and 2 were (0, $d/2$) m and (0, $-d/2$) respectively, where d ranged between 0 and 1 mm. It is important to note that this simulation is not a realistic star, but I chose these values since they were within the same orders of magnitude as the two source experiment.

To test the convergence of the phases, I reduced the number of distances calculated to 20 and I had those distance points range from 0 to .5 mm. I generated 3000 source points using the Fibonacci method and I set three different values for N_p: 100, 5000, and 10000 random phases.

3 Results and Discussion

3.1 Two Point Sources

Using the conditions that I described in Section 2.1, I graphed the intensity correlation in Figure 6. The simulated data points are a very good fit for the theoretical curve because $\chi^2_{99} = .018655$ (where there are 99 degrees of freedom) and $p \approx 1$. A p-value being equal to one shows that it is a very strong fit. Additionally, since a and b both equal 1, the coefficient in front of the cosine term is 1/2 and the data points do go 1/2 above and below 1.

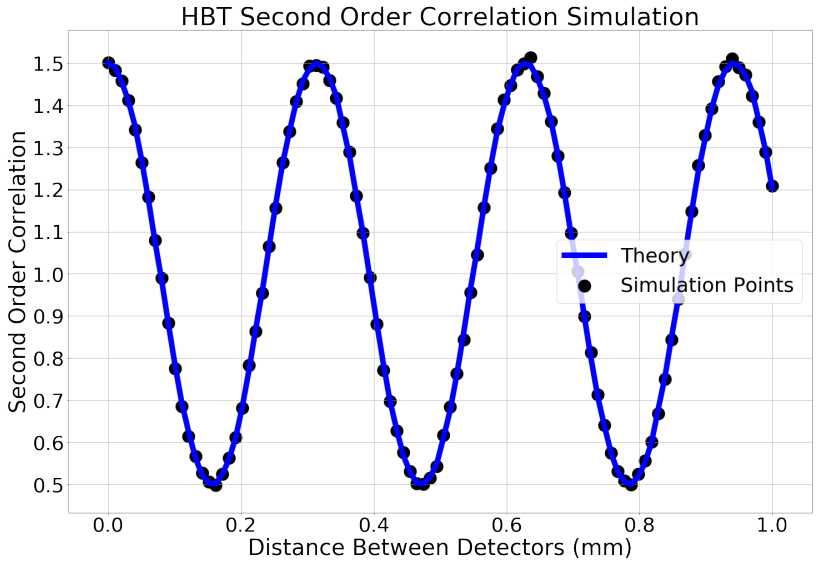

Figure 6: Two source simulation.

3.2 N_S Point Sources on a Star

3.2.1 Randomized Sources

Using the conditions that I mentioned in Section 2.2, I generated 1000 random points on the surface of a star. Figures 7 and 8 are a visual demonstration of what this looks like. Due to the randomization, the sources seem to be clustered in some areas and spread out in others.

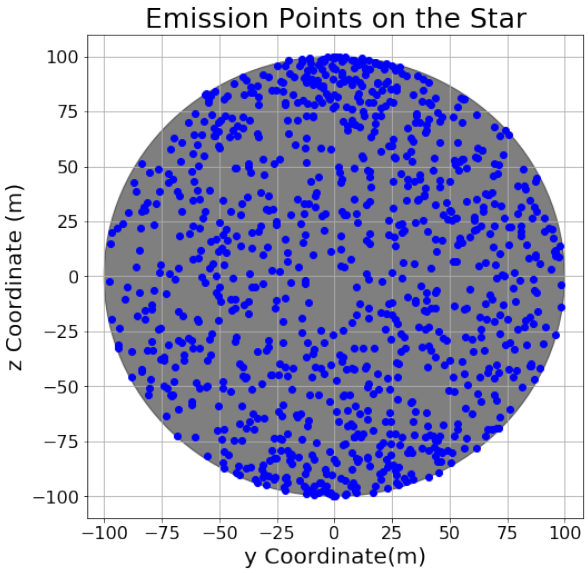

Figure 7: Emission points graphed on the z vs. y plane.

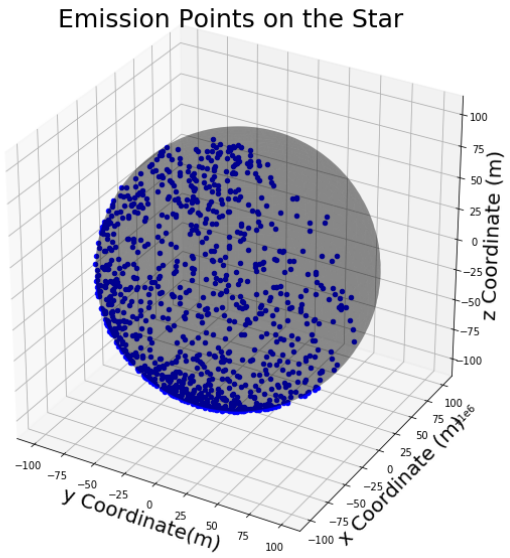

Figure 8: Sources in 3D space.

An important thing to note about the intensity correlation curve for a star, is that it first equates to two since all of the cosines have an argument of zero. Then, as d increases the cosine terms all start to destructively interfere with each other and there is a horizontal line of $y = 1$. My simulation demonstrates this very well (see Figure 9). The χ^2_{99} value for the theoretical and simulated data was .065 which had a corresponding p-value of ≈ 1. This shows that the simulated data nicely matched the theoretical line.

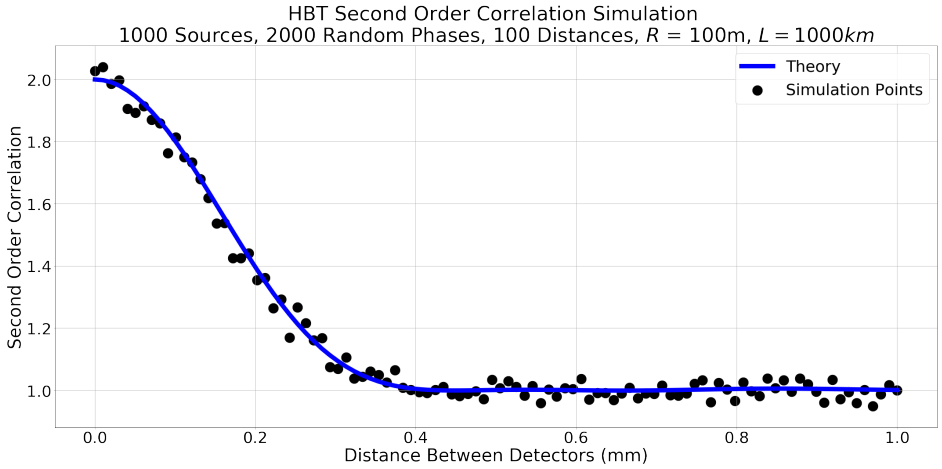

Figure 9: N_S source simulation plotted against theoretical curve.

The angular diameter of my simulated sphere is $2\tan(100/10^6) = 200$ μrads. Using Eq. 5, I fitted my simulated data to extract the angular diameter (see Figure 10). I got a value of 188.3 ± 1.7 μrads, which has a small relative error of 5.85%. The fit looks quite good, but it is still slightly off. The residual of the plot looks quite good since its slope is quite small and there is a small intercept (see Figure 11). Therefore, I think the fit is good.

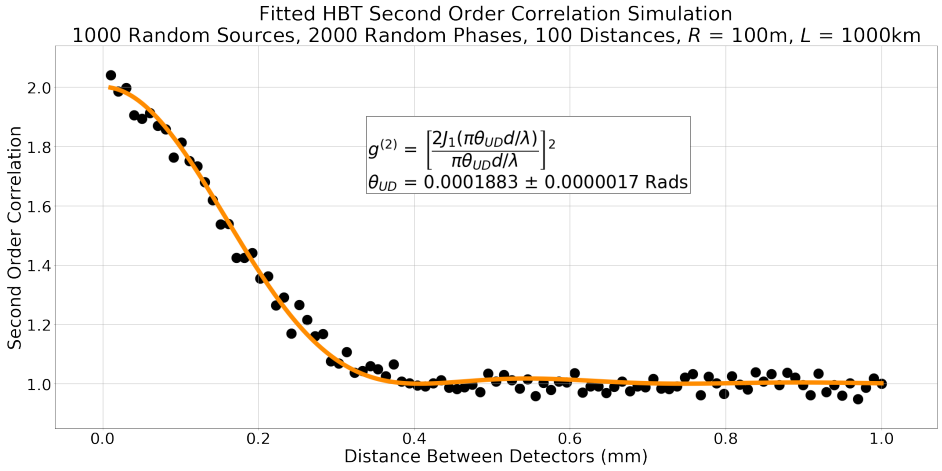

Figure 10: Fitted N_S source simulation for 1000 random sources.

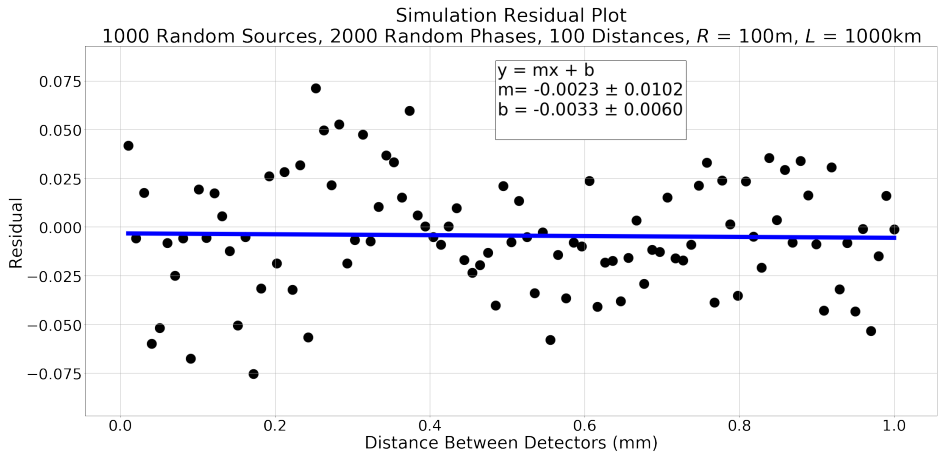

Figure 11: N_S source simulation for 1000 random sources residual.

I also fitted the theoretical values that I calculated using Eq. 29 (see Figure 12). I got a value of 184.32 ± .37 μrads, which is surprisingly smaller than what I found using the randomized phases. This value has a relative error of 7.84%. I also graphed the residual and the data seemed to oscillate around the x-axis to varying degrees (see Figure 13). Hence, I am doubtful of the quality of this fit.

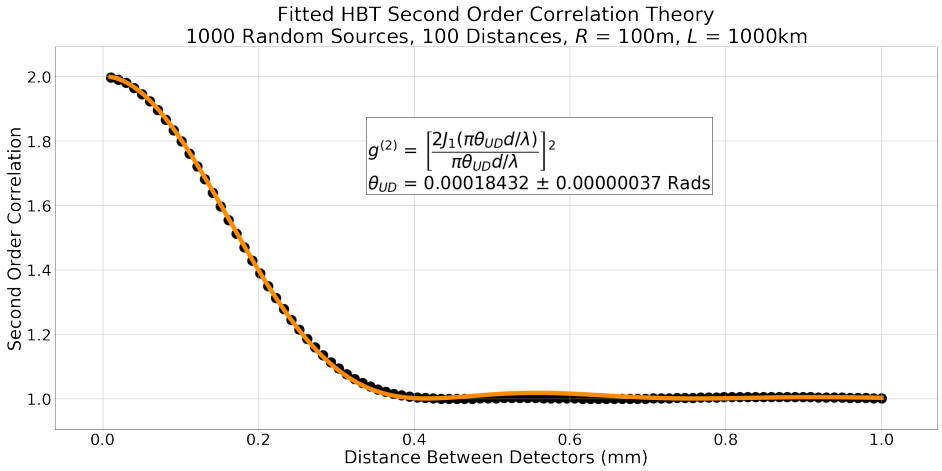

Figure 12: Fitted N_S source theory for 1000 random sources.

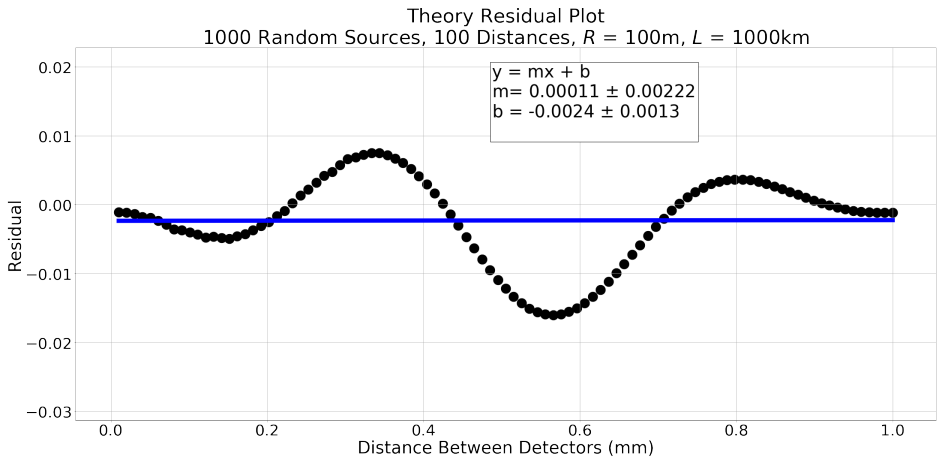

Figure 13: N_S source theory for 1000 random sources residual.

3.2.2 Equally Distributed Sources

Using the conditions that I established in Section 2.2, I generated 1000 roughly equidistant points on the surface of a star using a modified version of the Fibonacci sphere algorithm. Figures 14 and 15 are a visual demonstration of this technique. Notably, this method avoids the clustering problems present in randomized source generation.

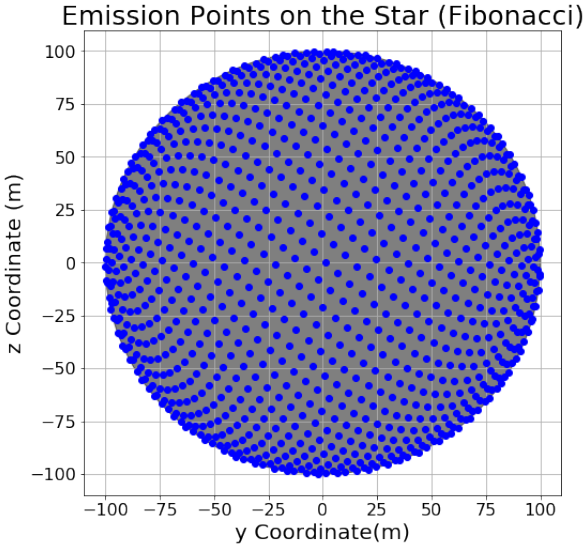

Figure 14: Emission points graphed on the z vs. y plane using the Fibonacci method.

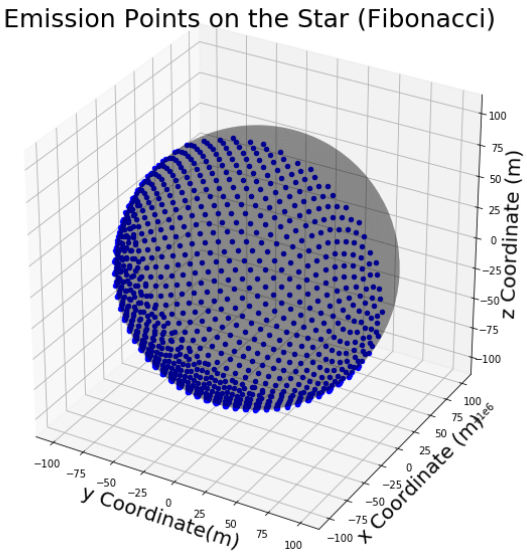

Figure 15: Sources in 3D space Fibonacci algorithm.

This simulation had a χ^2_{99} value of .051 which has a p-value of ≈ 1 (see Figure 16). Therefore, the theoretical curve is a very good fit for the simulated data points. It appears that the second maxima is

larger for this graph when compared to the randomized source simulation.

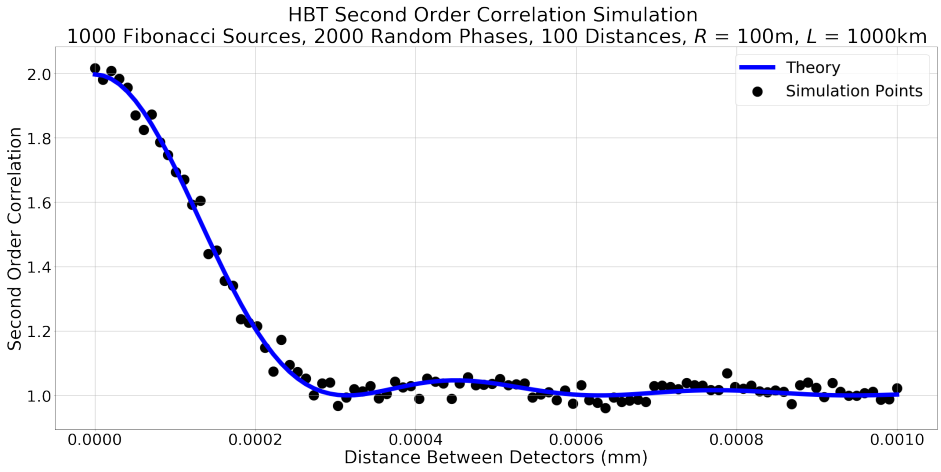

Figure 16: 1000 Fibonacci sources simulation plotted against theoretical curve.

As I did in the previous section, I fitted my simulated data to find the angular diameter (see Figure 17). I got a value of 233.5 $\pm$ 2.1 μrads, which has a relative error of 16.75%. The residual of the plot looks reasonable, but there is still a prominent upward trend in the data (see Figure 18). That being said, the fit seems decent.

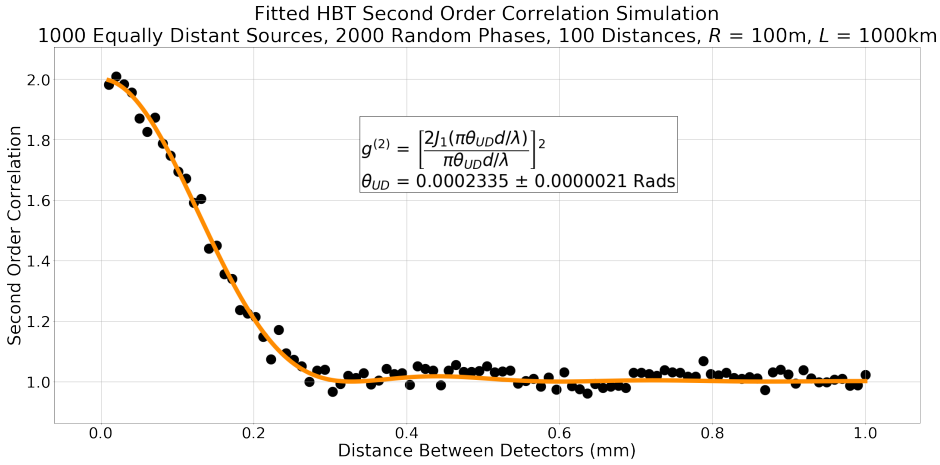

Figure 17: Fitted N_S source simulation for 1000 equidistant sources.

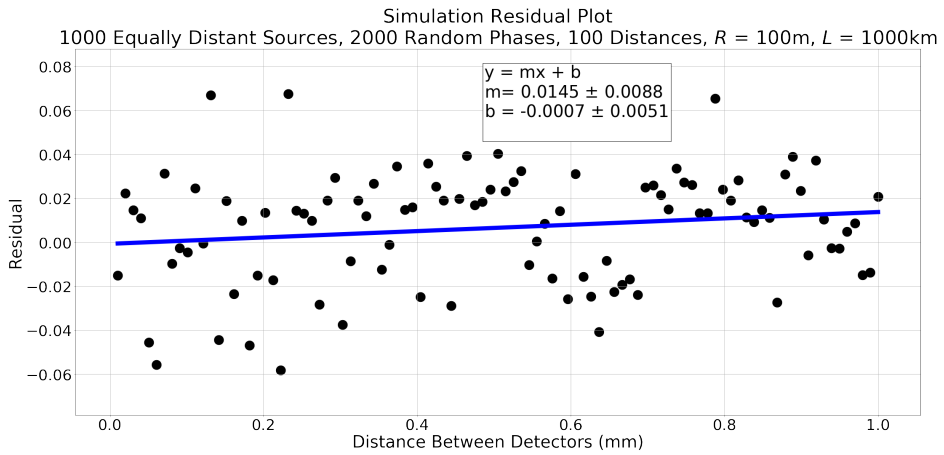

Figure 18: N_S source simulation for 1000 equidistant sources residual.

Additionally, I fitted the theoretical values that I calculated using Eq. 29 (see Figure 19). I got a value of 233.62 ± .89 μrads, which has a relative error of 16.81%. I also graphed the residual and like for the randomized source theory residual, the data points seemed to oscillate around the x-axis to varying degrees (see Figure 20). This makes me question the quality of this fit.

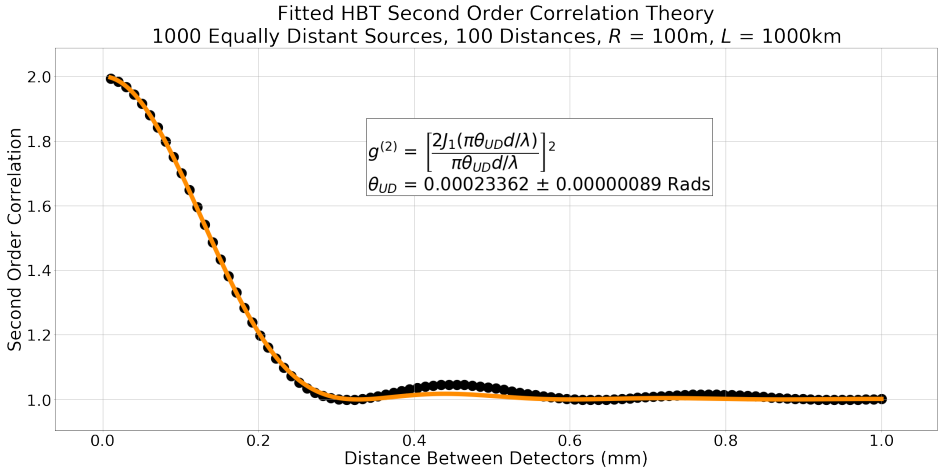

Figure 19: Fitted N_S source theory for 1000 random sources.

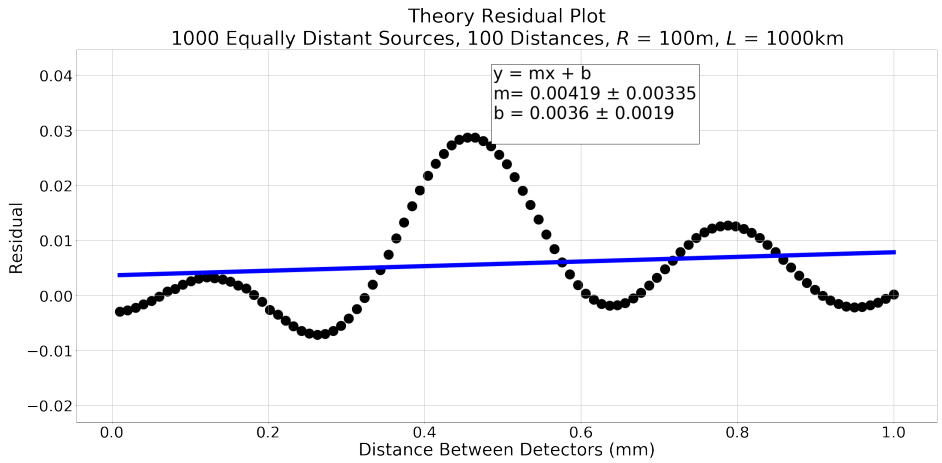

Figure 20: N_S source theory for 1000 random sources residual.

3.2.2.1 Phase Convergence Testing I have also tested if increasing the number of phases causes the data points to converge to the theoretical value. To do this, I increased the number of points I sampled from 1000 to 3000 (see Figure 21 & 22). I also used the Fibonacci sampling method because it would keep the points constant, which eliminates a source of error. To save on computational time, I calculated the correlations for 20 distances instead of 100 and I also halved the range of my data from [0, 1] mm to [0, .5] mm. Using these conditions, I found the correlations for three phase values: 100, 5000, and 10000.

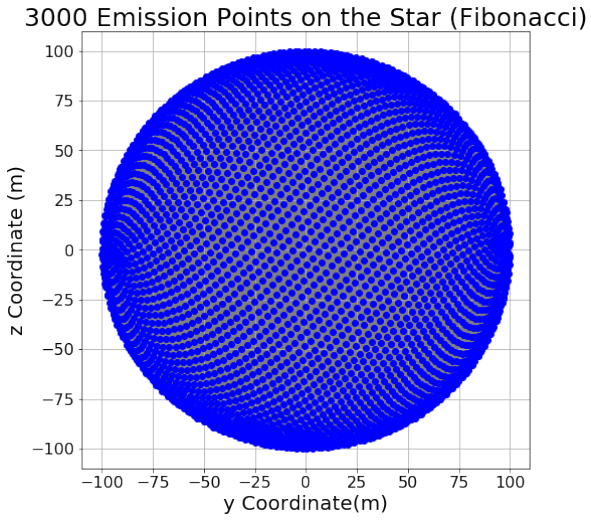

Figure 21: 3000 emission points graphed on the z vs. y plane using the Fibonacci method.

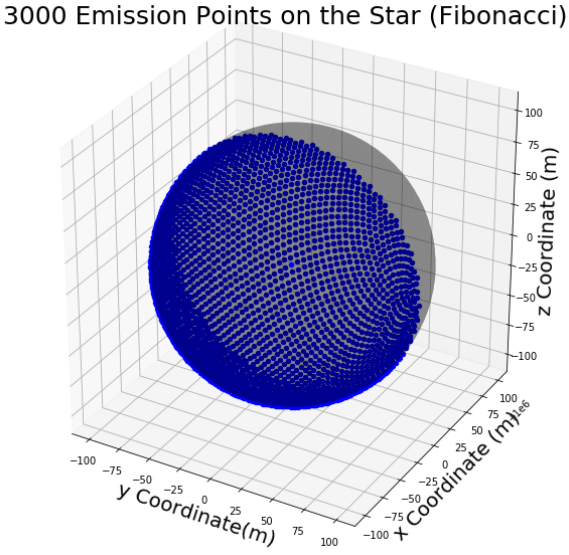

Figure 22: 3000 sources in 3D space using the Fibonacci method.

Figure 23, which used 100 phases, has a χ^2_{19} value of .28 and a p-value of ≈ 1. Despite this, the theoretical

values still match up decently with the simulated data.

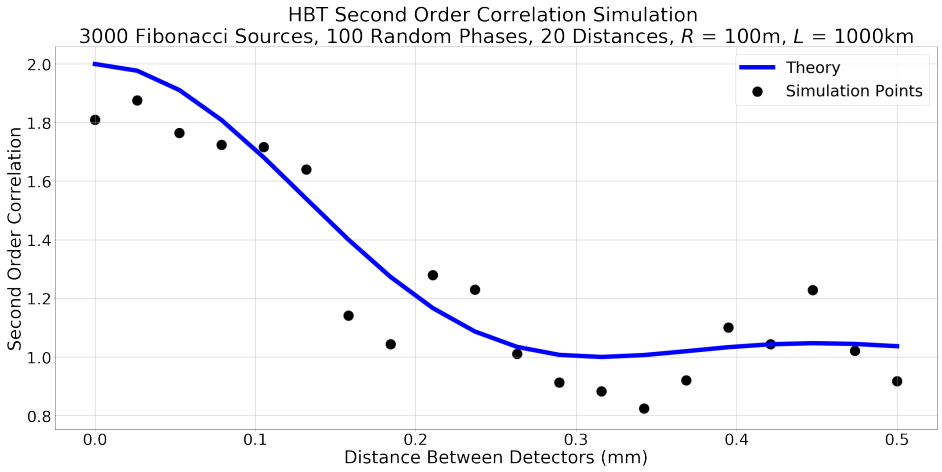

Figure 23: Simulation of 3000 evenly spaced sources and 100 phases.

Since the theoretical fit will be the same for all the variations of the phase, I only need to find the angular diameter using the theoretical fit once. I got an angular diameter of 233.7 $\pm$ 1.9 μrads, which has a relative error of 16.85% (see Figure 24). The residual has a significant slope and the data points are oscillating around the x-axis (see Figure 25). This leads me to doubt the quality of the fit.

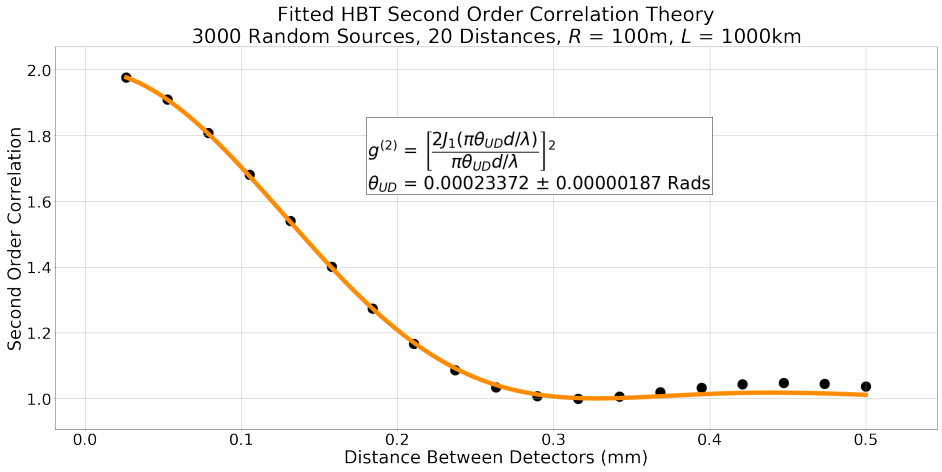

Figure 24: Fitted N_S source theory for 3000 random sources.

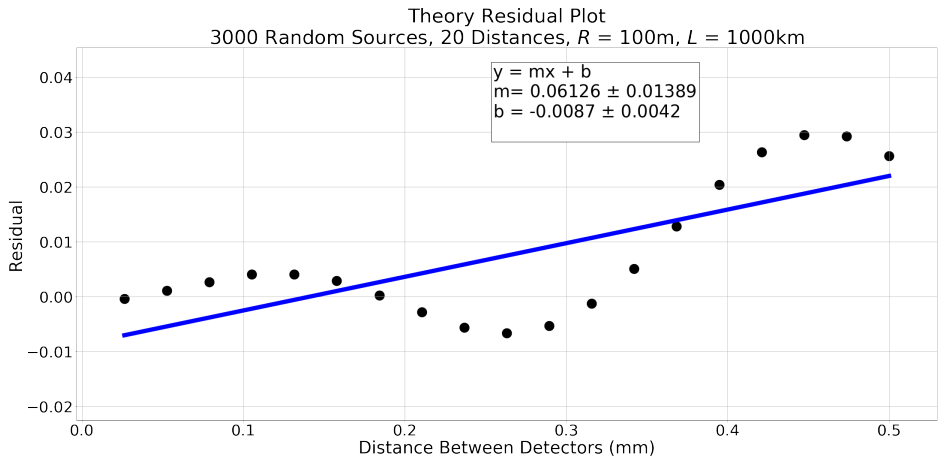

Figure 25: N_S source theory for 3000 random sources residual.

The fit for the simulated data points gave me an angular diameter of 250 $\pm$ 18 μrads which has a large relative error of 25% when compared to the expected value (see Figure 26). The residual has a significant upward trend and the magnitudes of the residuals are much larger than I have seen in previous simulations, which is why the absolute error of the angular diameter is an order of magnitude larger than I have previously observed (see Figure 27).

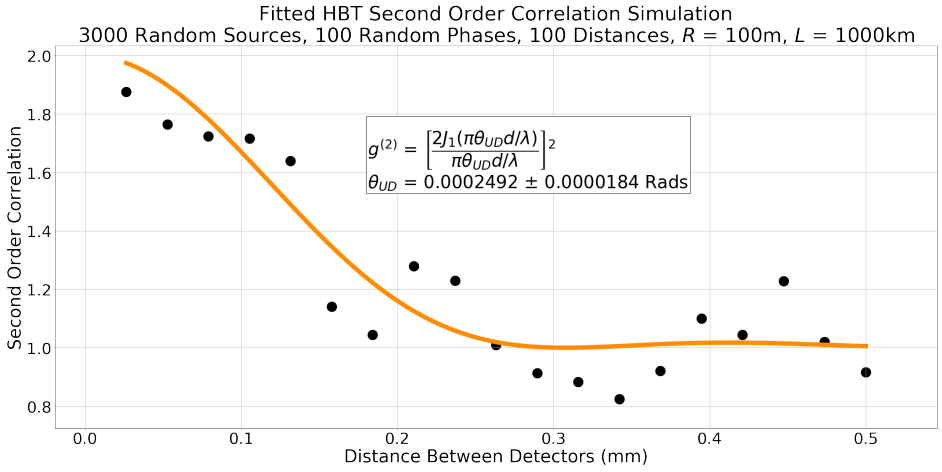

Figure 26: Fitted N_S source simulation for 3000 equidistant sources and 100 phases.

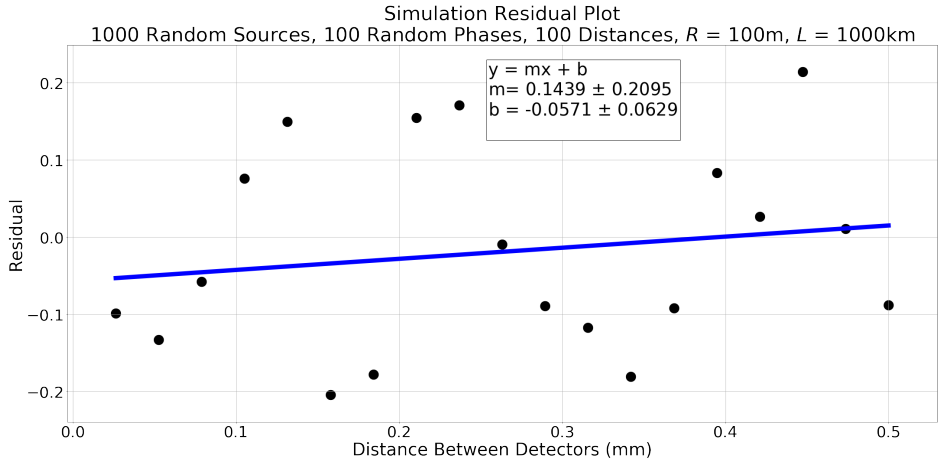

Figure 27: Residual for the simulation with 3000 equidistant sources and 100 phases.

The simulation with 5000 phases has a χ^2_{19} value of .004670 with a p-value that is ≈ 1 (see Figure 28). As such, the theoretical curve is a good fit.

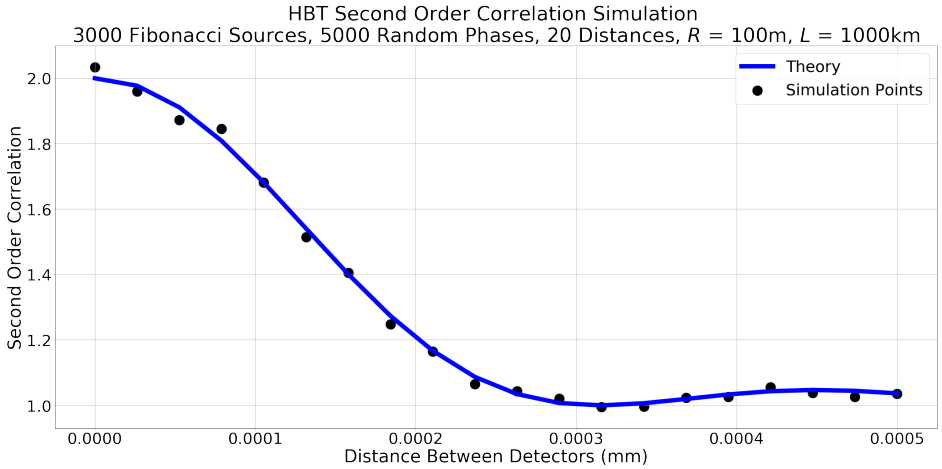

Figure 28: Simulation of 3000 evenly spaced sources and 5000 phases.

Fitting the simulated data points gave me an angular diameter of 236.4 ± 2.8 μrads (see Figure 29). This has a relative error of 18.2%. The residual of the data has a linear slope, but this slope is smaller than the 100 phase fit's slope, suggesting that this fit is better (see Figure 30).

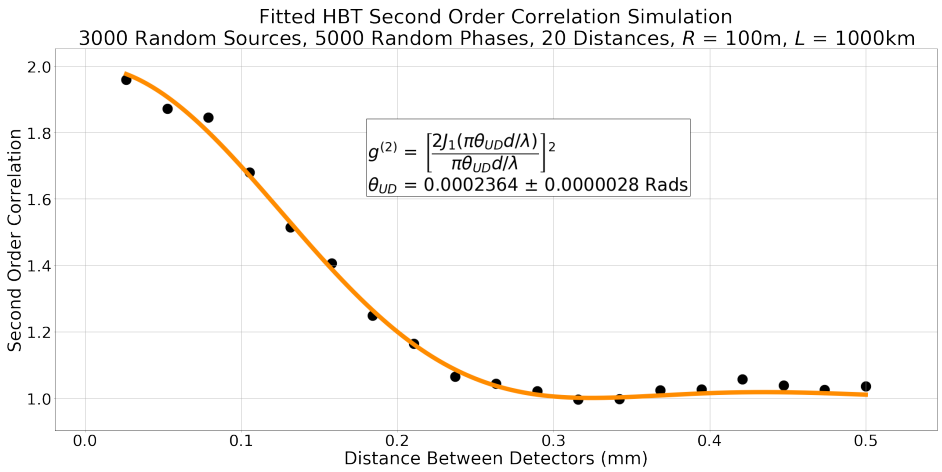

Figure 29: Fitted N_S source simulation for 3000 equidistant sources and 5000 phases.

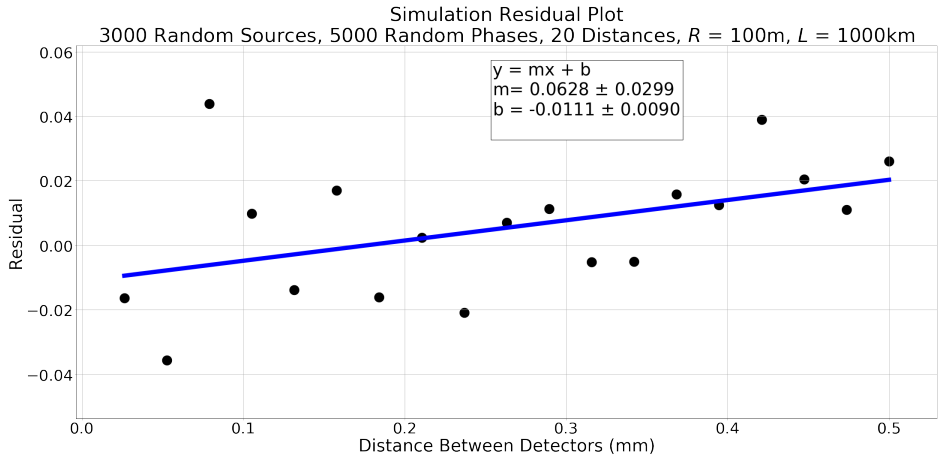

Figure 30: Residual for the simulation with 3000 equidistant sources and 5000 phases.

Lastly, the 10,000 phase simulation yielded a χ^2_{19} value of .00468 with a p-value that is ≈ 1, which means that the theoretical curve is a good fit (see Figure 31).

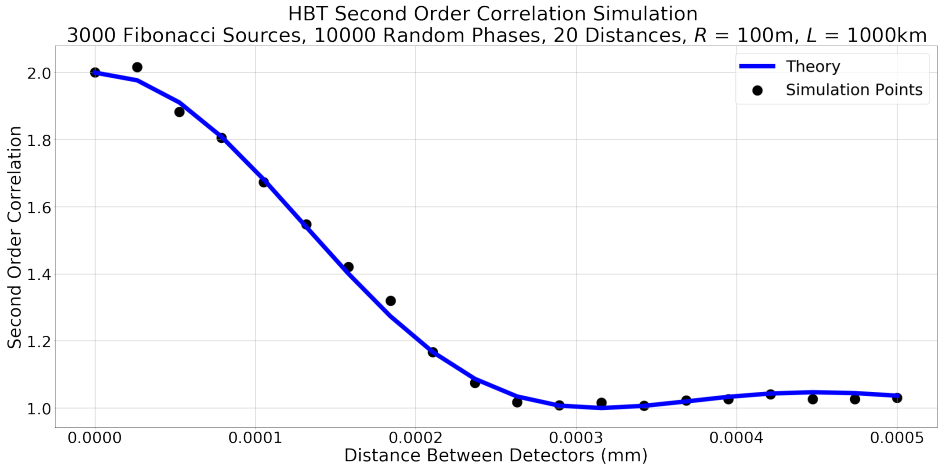

Figure 31: Simulation of 3000 evenly spaced sources and 5000 phases.

Fitting the simulated data points for this condition gave me an angular diameter of 231.2 $\pm$ 2.5 μrads (see Figure 32). This has a relative error of 15.6%. The residual of the data has a linear slope, but this slope is smaller than the 5000 phase fit's slope, meaning that this fit is better (see Figure 33).

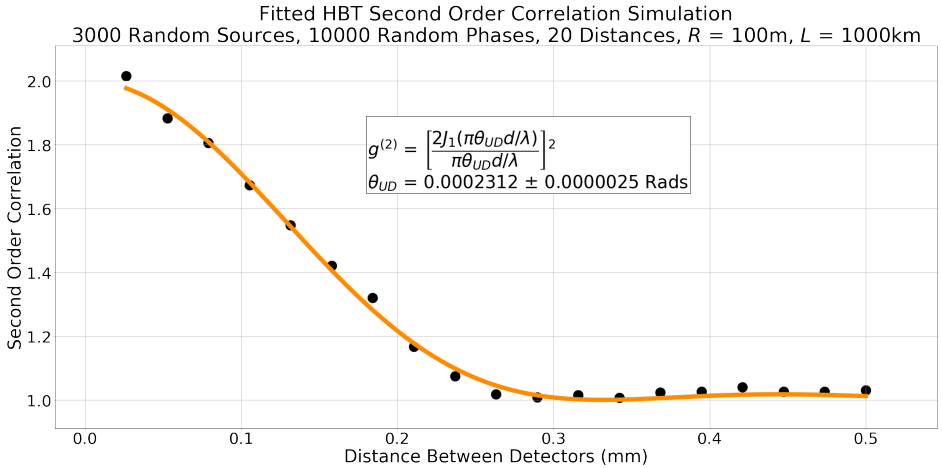

Figure 32: Fitted N_S source simulation for 3000 equidistant sources and 10000 phases.

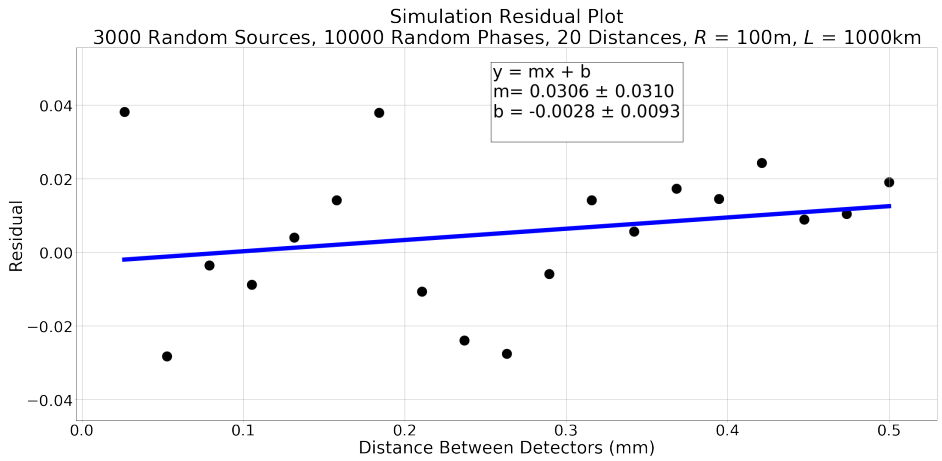

Figure 33: Residual for the simulation with 3000 equidistant sources and 10000 phases.

3.2.3 Discussion

A summary of my results for the different sources can be found in Table 1 and Table 3. A summary of the relative errors for the different sources can be found in Table 2 and Table 4. A summary of the fit statistics for the 3000 Fibonacci sources can be found in Table 5.

Summary of the N_S=1000 Sources Results

Data Type	Randomized Sources Angular Diameter (μrads)	Equidistant Sources Angular Diameter (μrads)
Simulation	188.3 ± 1.7	233.5 ± 2.1
Theory	184.32 ± .37	233.62 ± .89

Table 1: The summary of my 1000 sources results.

Summary of the N_S = 1000 Sources Relative Errors

Type	Randomized Sources Relative Error	Equidistant Sources Relative Error
Simulation	5.85%	16.75%
Theory	7.84%	16.81%

Table 2: The summary of my 1000 sources relative errors.

Summary of the N_S = 3000 Equidistant Sources Results

Type	Angular Diameter (μrads)
Theory	233.7 ± 1.9
N_p = 100	250 ± 18
N_p = 5000	236.4 ± 2.8
N_p = 10000	231.2 ± 2.5

Table 3: The summary of my 3000 equidistant sources results.

Summary of the $N_S = 3000$ Equidistant Sources Relative Errors

Type	Relative Error
Theory	16.85%
$N_p = 100$	25%
$N_p = 5000$	18.2%
$N_p = 10000$	15.6%

Table 4: The summary of my 3000 equidistant sources relative errors.

Summary of the Statistics for the $N_S = 3000$ Equidistant Sources

Number of Phases	χ^2_{19}	p-value
100	.28	≈ 1
5000	0.00470	≈ 1
10000	0.00468	≈ 1

Table 5: The summary of my 3000 equidistant sources statistics.

My results in Tables 1 & 2 are the opposite of what I would expect. I would think that the theoretical fits would be closer to the actual value of 200 μrads and that the equidistant sources would be closer to the actual value than the randomized sources. It also interesting that the randomized sources produce a value that is below the expected value and the equidistant sources produce a value that is above the expected result. I think this is just because of the specific point configuration that was generated and there are probably just as many randomized source configurations that would yield a result larger than the expected result.

The results in Tables 3 & 4 shows that as the number of phases increases, the measured angular diameter is closer to the actual value. Interestingly, the angular data that corresponds to the 10,000 phases has a smaller relative error than the theoretical curve. I think this may just be the randomness of the phases assisting the measurement and that there are probably other random configurations of phase that would negatively impact the relative error. Additionally, since the χ^2_{19} values in Table 5 are decreasing as the phase count is increasing, I can conclude that an infinite number of phases would converge to the theoretical value. However, since the p-values are all roughly the same there aren't any major significant differences between the three phases.

Another interesting observation is that the 3000 equidistant source star's fitted theoretical angular diameter has a slightly larger relative error than the 1000 equidistant source star's fitted theoretical angular diameter. I am unsure as to why this is, although there are a variety of possible reasons that all the angular diameters do not match the expected result more closely. For example, the approximation that the star is a circular disk could be causing a significant error. Similarly, my method of representing a star by placing N_S point sources on the surface of a hemisphere may not be entirely accurate. Another possible error is that I did not use enough source points in the simulation because stars are made up of many more atoms, which function as point emitters, than I could possibly simulate. Lastly, since I concluded that an infinite number

of phases converges to the theoretical value, a small sample of random phases cannot be a source of error since the theoretical values are still off.

4 Conclusion

The Hanbury Brown and Twiss experiments demonstrated the possibility and applicability of intensity correlations in the visible spectrum using PMTs. I have successfully derived the intensity correlation formulas for two and three source systems and I have further generalized those results for a system of N_S sources. I first tested these formulas by simulating the intensity correlations for a two source system where the simulated data points statistically matched the theoretical curve. I simulated the generalized formula by choosing data points on the surface of a star using two methods: randomly and using the Fibonacci Algorithm. Surprisingly, the random method proved to be more accurate, but I think that this is just because of the specific configuration of source points that was randomly chosen. Some other possible errors could be that the assumption that the star is a circular disk is not good, not sampling enough sources, and my model of the star may be inaccurate. I have also shown that increasing the number of randomized phases results in a decreased χ^2_{19} which means that an infinite number of phases would likely converge to the theoretical curve.

5 Acknowledgements

I'd like to make a special note that Abhishek Cherath and I worked together on the two point source simulation. I'd also like to thank Dr. Eric Jones, Dr. Marty Cohen, and Professor Harold Metcalf for their help and guidance in this project.

References

[1] Hanbury Brown, R., & Twiss, R. Q. "Correlation between Photons in two Coherent Beams of Light". In: *Nature* 177.4497 (1956), pp. 27–29. DOI: https://doi.org/10.1038/177027a0.

[2] Hanbury Brown, R., & Twiss, R. Q. "A Test of a New Type of Stellar Interferometer on Sirius." In: *Nature* 178.4497 (1956), pp. 1046–1048. DOI: https://doi.org/10.1038/1781046a0.

[3] Hanbury Brown, R., & Twiss, R. Q. "Interferometry of the intensity fluctuations in light - I. Basic theory: the correlation between photons in coherent beams of radiation". In: *Royal Publishing Society* 242 (1957), pp. 300–324. DOI: https://doi.org/10.1098/rspa.1957.0177.

[4] Grant R. Fowles. *Introduction to Modern Optics*. 2nd ed. New York, USA: Dover Publications, inc., 1989.

[5] Gordon, B. "The physics of Hanbury Brown–Twiss intensity interferometry: from stars to nuclear collisions". In: *Acta Physica Polonica B* 29 (1998), pp. 1839–1884. URL: https://arxiv.org/abs/nucl-th/9804026v2.

[6] R. Hanbury Brown and R. Q. Twiss. "The Question of Correlation between Photons in Coherent Light Rays". In: *Nature* 178.4548 (Dec. 1, 1956), pp. 1447–1448. ISSN: 1476-4687. DOI: 10.1038/1781447a0. URL: https://doi.org/10.1038/1781447a0.

[7] Hanbury Brown, R., & Twiss, R. Q. "The Question of Correlation between Photons in Coherent Beams of Light". In: *Nature* 179.4570 (1957), pp. 1128–1129. DOI: https://doi.org/10.1038/1791128a0.

[8] *Evenly distributing n points on a sphere*. URL: https://stackoverflow.com/questions/9600801/evenly-distributing-n-points-on-a-sphere.